43 is overexpressed in human fetal membrane defects after fetoscopic surgery

Short version of title: Abnormal Cx43 in fetal membrane defect.

David W. Barrett[1], Anna L. David[2], Christopher Thrasivoulou[3], Alvaro Mata[1], David L. Becker[4], Alex C. Engels[5], Jan A. Deprest[5], Tina T. Chowdhury[1, *]

[1]Institute of Bioengineering, School of Engineering and Materials Science, Queen Mary University of London, Mile End Road, London E1 4NS, UK.

[2]Institute for Women's Health, University College London, 86-96 Chenies Mews, London WC1E 6HX, UK.

[3]Department of Cell and Developmental Biology, University College London, Gower Street, London WC1E 6BT, UK.

[4]Lee Kong Chian School of Medicine, Nanyang Technological University, 11 Mandalay Road, Singapore.

[5]Department of Obstetrics and Gynaecology, University Hospitals Leuven, Leuven, Belgium.

Corresponding author: Dr Tina Chowdhury, Institute of Bioengineering, School of Engineering and Material Science, Queen Mary University of London, Mile End Road, London, E1 4NS. Tel: +44 0207 8827560. Email address: t.t.chowdhury@qmul.ac.uk

Conflict of interest: The authors report no conflict of interest and no financial interest.

Word count: abstract (200); main text (3795**).**

What's already known about this topic? After fetoscopic surgery, the fetal membrane fails to heal spontaneously and the membrane defect is prone to iatrogenic PPROM.

What does this study add?
- We observed abnormal connexin 43 expression in the wound edge with preferential distribution in the mesenchymal cells compared to the epithelial cells.
- The overexpression of Cx43 may interfere with normal healing of the amniotic membrane after fetoscopic surgery.

Abstract

Objective: We examined whether surgically induced membrane defects elevate connexin 43 (Cx43) expression in the wound edge of the amniotic membrane (AM) and drives structural changes in collagen that affects healing after fetoscopic surgery.

Method: Cell morphology and collagen microstructure was investigated by SEM and SHG in fetal membranes taken from women who underwent fetal surgery. IMF and RT-qPCR was used to examine Cx43 expression in control and wound edge AM.

Results: SEM showed dense, helical patterns of collagen fibrils in the wound edge of the fetal membrane. This arrangement changed in the fibroblast layer with evidence of collagen fibrils that were highly polarised along the wound edge but not in control membranes. Cx43 was increased by 112.9% in wound edge AM compared to controls (p<0.001), with preferential distribution in the fibroblast layer compared to the epithelial layer (p<0.01). In wound edge AM, mesenchymal cells had a flattened morphology and there was evidence of poor epithelial migration across the defect. Cx43 and COX-2 expression was significantly increased in wound edge AM compared to controls (p<0.001).

Conclusion: Overexpression of Cx43 in the AM after fetal surgery induces morphological and structural changes in the collagenous matrix that may interfere with normal healing mechanisms.

Keywords: Connexin 43, collagen, amniotic membrane; preterm premature rupture of the membrane.

Introduction

Mechanical rupture of the fetal membranes can occur as a result of trauma and after invasive prenatal interventions such as open fetal surgery, fetoscopy or amniocentesis leading to iatrogenic pre-term premature rupture of the fetal membrane (PPROM). The demand for fetal surgery is increasing as it has become evident that in some conditions, treatment *in utero* improves long term outcome. Fetoscopic laser ablation is now routinely performed for advanced twin-to-twin transfusion syndrome (TTTS) and fetal repair of congenital myelomeningocele has been shown to improve motor function postnatally.[1,2] However, spontaneous healing of the defect in the amniotic membrane (AM) does not occur after fetoscopic surgery and a visible membrane defect is left which is prone to rupture.[3-5] PPROM complicates over 30% of fetal surgeries that are being used to treat abnormalities in the unborn baby. However, PPROM and subsequent preterm birth compromises the outcome of treated babies, reducing the clinical effectiveness of fetal surgery. There are no clinical solutions to improve healing of the fetal membranes after they rupture.[6-8]

Histologically, the fetal membranes consist of several distinctive layers and cell types within a 3D extracellular matrix network. The epithelial layer is the outermost layer of the fetal membrane and is composed of amniotic epithelial cells that secrete collagen types III and IV that form the basement membrane. The fibroblast layer is the thickest layer and consists of mesenchymal cells that secrete types I and III collagen to form the compact and spongy layers of the AM. Although the chorion is thicker than the AM, this tissue has greater tensile strength. However, it has been reported that repeated stretching of the amniochorion reduces the viscoelastic nature of the tissue, making it more susceptible to rupture.[9,10] This loss in mechanical resistance has been attributed to alterations in the collagen network within the compact, fibroblast and spongy layers of the AM which is why the tissue ruptures first.[9,11-13] The pathological mechanisms that cause collagen disruption in the AM involve

multiple pathways that increase production of cytokines, matrix metalloproteinases (MMPs) and/or prostaglandins.[14-17] In animal models, tensile stretch increased myometrial expression of inflammatory factors involving cyclo-oxygenase-2 (COX-2), the oxytocin receptor and the gap junction protein, connexin-43 (Cx43).[18-20] In human amniotic epithelial cells, application of 11% static stretch, induced activation of NF-κB and AP-1 leading to expression of COX-2, MMPs and prostaglandin E_2 (PGE_2) production.[21] Similarly, repetitive strain in human AM induced an inflammatory response, leading to tissue softening caused by alterations in proteoglycan, collagen and elastin content.[22-28] We observed that cyclic tensile strain of human AM increased expression of Cx43.[28] This important contractile responsive protein is a candidate upstream regulator of PGE_2 that affects cell migration, proliferation and matrix organisation. Overexpression of Cx43 plays a central role in preventing the wound healing response in human diabetic wounds and venous leg ulcers.[29,30] We hypothesise that Cx43 could regulate cell function and matrix composition in the AM after iatrogenic trauma, and promote remodelling mechanisms that interfere with the repair process and compromise fetal membrane integrity. The present study examined whether surgically induced membrane defects after fetoscopic surgery increase Cx43 expression in the wound edge of the AM and drives structural changes in collagen architecture.

Methods

Patient recruitment and sample collection: Human placentas (n=12) were collected after caesarean section after written informed consent from women who had undergone fetal surgery at University College Hospital London and the University Hospitals of Leuven, Belgium. Ethical approval was granted by the Joint UCL/UCLH Committees on the Ethics of Human Research (Ref: 08/H0714/87) and the Ethics Committee at the KU Leuven (Ref: P008-2011). Women underwent fetoscopic surgery for treatment of TTTS (n=10), fetal

congenital diaphragmatic hernia (CDH, n=1) and twin reversed arterial perfusion sequence. (TRAPS, n=1). Fetal surgical procedures were performed between 15+0 and 28+1 weeks of gestation and between 1 to 145 days before birth (Table 1). During the surgery, the fetoscopic entry site was created by using a 10-Fr Teflon cannula (Cook Medical, Strombeek Bever, Belgium) and pyramidal trocar device (Karl Storz, Tuttlingen, Germany). At delivery, the fetoscopic defect site was identified by careful macroscopic survey of the fetal membrane and the tissue around the wound was carefully excised. For the open fetal surgery case, the hysterotomy wound was excised as part of the routine entry into the uterus at caesarean section, and then the membranes were stripped from the overlying myometrium. A control region in the fetal membrane that was aligned in the same axis as the fetal defect and was at least 5 cm away from the wound edge was excised along with 2 cm margins of full thickness membrane. Excess maternal blood was removed by washing the fetal membrane specimens (5x5 cm) with Earle's Balanced Salt Solution (EBSS) for 2 min (Sigma-Aldrich, UK). Control and wound edge fetal membrane specimens were immediately fixed in 4% paraformaldehyde (PFA) for 2 hours and stored in PBS prior to analysis by scanning electron microscopy (SEM). In addition, the AM was separated from the chorionic membrane (CM) by gentle traction. The control and wound edge AM specimens were either fixed in 4% PFA for 2 hours or stored in RNA Later (Qiagen, Manchester, UK) prior to imaging and gene expression analysis, respectively.

Fetal membrane characterisation: SEM was used to evaluate the morphological characteristics of the AM and CM after fetoscopic interventions in wound edge specimens. Following fixation, the fetal membranes were washed with Milli-Q® water before being passed through a graded ethanol series and then critical point dried (K850, Quorum Technologies, UK). The tissue specimens were mounted on 10 mm SEM mounting blocks

and sputter coated with 30 nm gold particles before SEM analysis of the AM and CM (FEI Inspect™-F50, The Netherlands).

Immunostaining: Immunostaining was performed with whole-mount control and wound edge AM specimens that had been fixed in 4% PFA. The AM tissue specimens were washed twice in PBS for 5 min and with 0.1 M Lysine and 0.1% Triton X100 in PBS for 40 min. Specimens were blocked for 1 hour using 1% goat serum with PBS + 0.1% Triton X100. Primary antibodies for Cx43 (diluted 1:4000; Sigma, 6219) were incubated at room temperature overnight, as described (Wang CM, 2007). The tissues were washed with PBS and incubated with goat Alexa488 anti-rabbit secondary antibody for 2 hours at room temperature (1:400, Life Technologies). Secondary antibody incubation in the absence of primary antibody was used as a negative control. Tissues were counterstained for 20 min with 1 μg/ml of the nuclear dye DAPI (1:1000).

Second Harmonic Generation and confocal imaging: Control and wound edge AM specimens were imaged by two-photon confocal imaging on Leica SP8 with Coherent Chameleon Ultra, Ti Sapphire mode-locked IR laser, as previously described.[31] Briefly, Cx43 and Second Harmonic Generation (SHG) imaging was performed at 920 nm excitation, 25x 0.95 NA water immersion objective. The Cx43 signal was collected with the non-descanned external HyD detector through a FITC emission filter (500-550 nm barrier filter). The collagen SHG signal was collected via the transmission detector and 450-470nm barrier filter. The DAPI signal was collected sequentially with 405 nm excitation to avoid bleed through of nuclear signal into the Cx43 signal and emission signal via the confocal pin-hole to the de-scanned HyD detector between 400-490 nm. Approximately 150 micron volumes were acquired through the whole thickness of the samples at 1.2 μm z-section intervals. Maximum

brightness projections were performed of the whole z-stack. Parameters for laser power, detector gain and off-set were kept constant for each sample so that direct comparisons of the 8 bit digital images could be made per patient to permit quantification.

Image quantification and quantitative analysis: To characterise the direction of collagen alignment, an orientation distribution analysis using the directionality ImageJ plugin was performed. SHG images were converted to binary and 2D orientation analysis calculated using the local gradient orientation method. Cx43 immunostaining levels was quantitatively evaluated per tissue area using a well-established pixel-counting method.[32] The images were converted to binary images using identical threshold values and objects exceeding 2 pixels were counted to identify Cx43 positive pixels per tissue area (μm^2) or per cell nuclei. For quantification of Cx43 plaque density, the values for fluorescence intensity were converted to height using the Image J interactive 3D surface plot plugin, where each spike represents a Cx43 plaque.

Real-time quantitative PCR: Total RNA was extracted from control and wound edge AM specimens using Trizol reagent and purified using RNeasy Mini Kit (Qiagen, Manchester, UK). RNA was treated with DNA-free DNase for 20 min (Ambion Applied Biosystems, Warrington, UK). 200 ng of total RNA was reverse transcribed using Enhanced Avian RT First Strand cDNA synthesis kit with oligo(dT)$_{23}$ primer (Sigma Genosys, Cambridge, UK). For real-time RT-qPCR, each reaction was run in duplicate on a 96-well plate containing 5 μl SYBR green mastermix, 2.5 μl cDNA, and 2.5 μl primer pairs. The following specific primer sequences were used: Cx43 sense: 5'-CTCGCCTATGTCTCCTCCTG-3', antisense: 5'-TTGCTCACTTGCTTGCTTGT-3'; COL1A1 sense: 5'-CCCCGAGGCTCTGAAGGT-3', antisense: 5'-CACCAGCAATACCAGGAGCA-3'; COX-2 sense: 5'-

GGACAGGATTCTATGGAG-3', antisense: 5'-GGATGTCAACACATAACTC-3'; GAPDH

sense: 5'-TCTCTGCTCCTCCTGTTC-3'; and antisense: 5'-CGCCCAATACGACCAAAT-

3' (Sigma Genosys, Cambridge, UK). The Mx3000P quantitative PCR instrument was used

for real-time detection of PCR products (Stratagene, Amsterdam, The Netherlands).

Thermocycling conditions were 95°C for 2 minutes, followed by denaturation of 40 cycles at

95°C for 15 seconds, annealing at 60°C for 1 minute, and extension at 72$^{\text{o}}$C for 1 minute.

PCR efficiencies for optimal primer pair concentrations were derived from standard curves (n

= 3) by preparing a 10-fold serial dilution of cDNA from a sample that represented the

control. The real-time PCR efficiencies (E) of amplification for Cx43 was defined according

to the relation, $E = 10^{[-1/\text{slope}]}$. The R^2 value of the standard curve exceeded 0.99 and revealed

efficiency values ranging from 1.98 to 2 (98-100%). Primer specificity was verified by

examining the melting curve. Relative quantification of Cx43 was estimated by normalizing

the target to the reference gene, GAPDH, and to the calibrator sample (patient matched

control AM) by a comparative C_t approach. For each sample, the ratio of target ΔCt and

reference ΔCt was calculated, as previously described. [33-34] Ratios were expressed on a

logarithmic scale (arbitrary units).

Statistical analysis: Two-way Analysis of Variance (ANOVA) and the *post hoc* Bonferroni-

corrected *t*-test were used to examine data for Cx43 protein and gene expression in control

and wound edge AM. The number of replicates per patient for the control and wound edge

AM are indicated in the figure legend. In all cases, a level of 5% was considered

statistically significant ($p<0.05$).

Results

Morphology of the fetal membranes after fetoscopic surgery: Figure 1 shows there was no growth of tissue into the fetal membrane defect even 71 days after its creation. Instead, the wound edge was found to roll, resulting in an irregular wound size of approximately 3 mm diameter (Figure 1). The fetal defect site showed densely, packed, helical patterns of collagen fibrils in the AM and CM, with no preferential direction. In some cases, thinner and longer length fibres were observed in the CM (indicated by white arrow, Figure 1), but the microstructure mainly consisted of a discrete network of collagen along the wound edge. At higher magnification (right panel), the fibres appeared loose and randomly aligned in the matrix with some fibres that were intermingled (indicate by white dotted arrow; Figure 1).

Collagen organisation in the fetal membrane defect: Control and wound edge specimens were examined by SHG confocal microscopy to compare collagen structure in the matrix region of the AM following fetoscopic surgery. Figure 2 shows representative images of the AM wound edge region with evidence of collagen fibril bundle organisation in the basement membrane and compact layer (indicated by white dashed arrows). In contrast, this arrangement changes within the fibroblast and spongy layer with evidence of collagen fibrils that are much more organised and aligned in parallel to the axis of the wound edge. In the fibroblast and spongy layer, the formation of the collagen fibres appear dense, elongated and highly aligned (white dashed inset, Figure 2) with evidence of greater intensity of the SHG signal within a 100 μm region closest to the wound edge (indicated by white lines). The direction of collagen fibre organisation showed a region of highly polarised fibres in all regions of the wound edge with a spread of ~0° (Fig. 3). This collagen structure appears to be more coherent and presents a different profile to control AM specimens where the fibre arrangement appears disorganised and is interwoven in a more or less random/loose fashion (Figure 3).

Changes in cell behaviour, Cx43 expression and collagen organisation: Our method of analysis by SHG in wound edge specimens used double imaging to examine qualitative changes in Cx43 protein expression by immunostaining of amniotic epithelial cells present in the epithelial layer and compared to mesenchymal cells present in the fibroblast layer, with nuclei counterstained with DAPI (Figure 4). In control AM, we visually observed low levels of Cx43 in regions within the epithelial and fibroblast layers (Figure 4). Quantitative analysis showed that the Cx43 signal was largely distributed in the fibroblast layer compared to the epithelial layer (all $p<0.001$), with values ranging from 543.1 μm^2 (stage 2) to 1818.6 μm^2 (stage IV) for control AM (Figure 5A). In wound edge AM, a significantly greater proportion of total tissue area was occupied by Cx43 in the fibroblast layer with values that progressively increased with disease state (2479.5 to 8175.8 μm^2; all $p<0.01$). Furthermore, mesenchymal cells present in wounded AM showed a striking upregulation of Cx43 per cell nuclei compared to patient matched controls (all $p<0.01$; Figure 5A), with negligible difference between diseased state. Integrated density analysis showed a significant increase of Cx43 protein expression in wound edge AM specimens (112.9%) compared to patient matched controls ($p<0.001$). IMF confocal microscopy showed typical punctate plaques of Cx43 localised at the sites of cell-cell contacts with greater number of plaques distributed in the wounded fibroblast layer (Fig. 5C) compared to control AM (inset). Gene expression of Cx43 and COX-2 was significantly increased in wounded AM compared to patient matched controls and was paralleled with an associated reduction in Type I collagen (all $p<0.001$; Figure 6). We did not observe significant differences in gene expression for control AM taken from individuals from the TTTS patient groups.

To better understand the changes in cell behaviour and collagen organisation, we observed a thickened bulb region of amniotic epithelial cells with evidence of cell migration that formed a cell mass close to the wound edge (white dashed arrow, Figure 7A, B).

Analysis by SEM showed a flattened mesenchymal cell morphology in the wounded fibroblast layer with characteristic lamellipodium projections (indicated by white arrows, Figure 7A inset) compared to a rounded-like cell phenotype in control AM (Figure 7C). At higher magnification, we observed highly aligned collagen fibres dispersed with flattened mesenchymal cells along the wound edge (Figure 7E, F). In contrast, the arrangement of collagen in patient matched control AM was compact, irregular and basket-like (Figure 7D).

Discussion

Defects in the fetal membranes created by fetal surgery are a significant problem that limits the effectiveness of a variety of fetal surgical treatments. Several studies have shown that membrane damage caused by the insertion of a needle or fetoscope leads to inflammation and elevated levels of pro-inflammatory cytokines, MMPs or C-reactive protein.[35] Histological studies have shown that wound repair is poor or absent in the fetal membranes making the tissue less able to provide mechanical support.[36-37] This affects the signalling triggered by mechanotransduction leading to major structural changes in the collagenous matrix as full term approaches.[13] Thus, mechanisms to stimulate wound closure and repair of matrix tissues in the membranes are needed to withstand the effects of increased tension and prevent premature rupture. However, the pathological mechanisms that lead to diminished collagenous matrix synthesis and impair wound healing in fetal membranes are poorly understood. It is well established that overexpression of Cx43 reduced fibroblast migration and the healing response in diabetic skin and venous leg ulcers, but no study to date has explored whether this gap junction protein is expressed in the fetal AM and interferes with normal cell migration and collagen organisation across the defect.

The present study showed a striking upregulation of Cx43 in the wound edge of the AM defect after fetoscopic surgery, compared to patient matched control AM specimens

taken 5cm away from the site of trauma. This was accompanied by changes in cell morphology and augmented collagen deposition close to the wound edge, with distinct differences in Cx43 expression in the epithelial and fibroblast layer. Even with a small homogenous group of ten TTTS patients, we observed a significant upregulation of Cx43 that was dependent on disease state and may prevent efficient healing of the AM. However, our observations need to be studied in large groups of patients and with much more detail of the variables (eg. maternal age, latency period, tissue location) that may influence membrane healing. Indeed, Papanna et al used histology and immunohistochemistry techniques to compare the changes of the fetal membranes at the trocar insertion site with distance and observed differences in cell death, autophagy and structural integrity for fetal membranes taken from TTTS patients. The collagen architecture was severely altered in the referenced membranes and also in the recipient's fetal membranes. Since we did not examine these phenomena in *control* specimens taken at great distance away from the defect, it is difficult to determine the mechanism in the fetal membranes taken from different sites.[38] Nevertheless, our observations in the human fetal AM are supported by evidence from animal models which showed elevated expression of Cx43 in the wound edge of diabetic rats.[39] In human diabetic foot ulcers, silencing Cx43 with antisense accelerated wound repair by improving fibroblast migration rates.[29] Using *in vitro* organ culture models, it was reported that mimetic peptides that target Cx43 could improve fibroblast and keratinocyte migration rates leading to wound closure.[40] Since it is possible to manipulate Cx43 expression, future studies should explore whether silencing of Cx43 in wounded membranes improves cell migration, with the aim to therapeutically control the self-repair process.

We also observed poor epithelial migration adjacent to the site of injury across the defect. The mesenchymal cells appeared flattened in the fibroblast layer and the epithelial cells crawled forward across the edge and formed a thickened bulb appearance, which may

represent an initial attempt by the cells to heal the wound. Indeed, the formation of a thin tongue at the wound edge is an early hallmark of healing indicating the start of re-epithelialisation. It is postulated that the efficiency of cell migration across the fetal defect could be influenced by the absence of factors that help the healing response. For example, cell proliferation and migration to the site of injury are regulated by integrins that activate physiological wound repair mechanisms. Although the regulation of integrins by tensile stretch in the AM is not known, apoptosis can result from the lack of integrin anchorage to the collagenous matrix.[41.42] Apoptosis and autophagy was observed in fetal membranes after fetoscopic surgery with histological changes that disrupt collagen structural integrity.[42] The overexpression of Cx43 observed in the present study may play a role in switching off normal integrin signals and upregulate cytokines and enzymes that drive collagen degradation, leading to membrane rupture. In addition, stretching of the fetal membrane *in vitro* upregulates a number of pro-inflammatory cytokines, chemokines and MMPs that trigger mechanotransduction and tissue remodelling and these mechanisms should be explored further.

The present study showed greater deposition of collagen in the fibroblast and spongy layer compared to the epithelial regions, with highly polarised fibre alignment along the axis of the wound edge. Cell morphology appeared flattened in the wound edge suggesting an attempt by mesenchymal cells to repair the tissue due to enhanced deposition of collagen along the axis of the fetal defect. This organization is reminiscent of embryonic wound healing where the wounds heal by contraction of an F-actin band that forms around the wound and contracts in a purse string like fashion.[44] In tenocytes subjected to tensile strain, there is evidence that Cx43 co-localises with actin filaments and influences tissue remodelling and growth.[45,46] This reparative attempt of tissue remodelling may not contribute to normal collagen deposition needed for robust fetal membranes that can withstand tensile

stretch during pregnancy. Indeed, previous *in vivo* models show that collagen structure can control the organisation of the connective tissue matrix. The remodelling phases of repair and arrangement of collagen fibres are dependent on the influence of mechanical forces that activate mechanotransduction pathways and modulate the quality of those fibres at the different levels of hierarchy.[20] We previously found that subjecting the human AM to cyclic tensile strained increased collagen alignment and was mediated by overexpression of Cx43. This response was associated with a reduction in tangent stiffness and weakening of the AM. In the present study, the resulting alignment of fibroblasts and collagen could reduce elasticity in the membranes which is less able to withstand the mechanical force along the wound edge. We did not determine the mechanical properties of the fetal membrane defect in this study due to limitations in the amount of tissue available for analysis. However, current mechanical approaches cannot easily separate the contribution of mechanical anisotropy due to the hierarchical arrangement of the collagen molecules in the fibril and/or parallel packing of fibrils in the tissue layers of the AM .[46-48] The mechanical properties of collagen fibrils have been measured by nanoindentation and atomic force microscopy,[49] suggesting that future studies which examine fibril stiffening due to cell migration should be investigated.

Conclusion

The present study showed increased expression of Cx43 in the fibroblast and spongy layer of the human AM after fetoscopic surgery. We observed highly aligned collagen fibres along the axis of the wound edge secreted by mesenchymal cells that increased collagen deposition in an initial attempt to repair the AM. We postulate this effect is achieved by directing collagen matrix alignment and spatial arrangement similar to tissues which have been subjected to tensile strain. However, the wound healing response is not sustainable long term and the molecular pathways activated by Cx43 to recruit matrix proteins and activate signalling

mechanisms for repair should be investigated. We provide evidence that Cx43 plays a role in the process of wound healing in the human fetal membrane after fetoscopic surgery implicating regulation of this gap junction protein in directing collagen alignment.

Acknowledgements

References

1. Slaghekke F, Lopriore E, Lewi L, *et al.* Fetoscopic laser coagulation of the vascular equator versus selective coagulation for twin-to-twin transfusion syndrome: An open-label randomised controlled trial. Lancet 2014;383(9935):2144–51.

2. Adzick NS, Thom EA, Spong CY, *et al*. A randomized trial of prenatal versus postnatal repair of myelomeningocoele. N Engl J Med 2011;364:993–1004.

3. Deprest, J, Van Schoubroeck, D, Van Ballaer, P *et al.* Alternative access for fetoscopic Nd:YAG laser in TTS with anterior placenta. US Obstet Gynecol 1998;347-55.

4. Gratacos E, Sanin-Blair J, Lewi L, et al. A histological study of fetoscopic membrane defects to document membrane healing. Placenta 2006; 27:452–6.

5. Mallik AS, Fichter MA, Rieder S, *et al*. Fetoscopic closure of punctured fetal membranes with acellular human amnion plugs in a rabbit model. Obstet Gynecol 2007;110(5):1121-9.

6. Deprest JA, Lerut TE, Vandenberghe K. Operative fetoscopy: new perspective in fetal therapy? Prenat Diagn 1997;17(13):1247–60.

7. Harrison MR. Surgically correctable fetal disease. Am J Surg. 2000;180(5):335-42.

8. Devlieger R, Millar LK, Bryant-Greenwood G, *et al.* Fetal membrane healing after spontaneous and iatrogenic membrane rupture: A review of current evidence. Am J Obstet Gynecol 2006;195(6):1512-20.

9. Parry-Jones E, Priya S. A study of the elasticity and tension of fetal membranes and the relation of the area of the gestational sac to the area of the uterine cavity. BJOG. 1976:83;205-212.

10. Lavery JP, Miller CE, Knight RD. The effect of labor on the rheologic response of chorioamniotic membranes. Obstet Gynecol. 1982;60(1):87-92.

11. Jabareen M, Mallik AS, Bilic G, *et al.* Relation between mechanical properties and microstructure of human fetal membranes: an attempt towards a quantitative analysis. Eur J Obstet Gynecol Reprod Biol 2009;144:S134-41.

12. Oyen M, Calvin SE, Cook RF. Uniaxial and biaxial mechanical behaviour of human amnion. Mater Res Soc Symp Proc 2005;844:161-166.

13. Helmig R, Oxlund H, Petersen LK, Uldbjerg N. Different biomechanical properties of human fetal membranes obtained before and after delivery. Eur J Obstet Gynecol Reprod Biol 1993;48:183-9.

14. Mercer BM. Preterm premature rupture of the membranes. Neuro Endocrinol Lett 2008;29(2):205-21.

15. Skinner KA, Challis JR. Changes in the synthesis and metabolism of prostaglandins by human fetal membranes and decidua at labour. Am J Obstet Gynaecol 1985;151:519–523.

16. Devlieger R, Deprest JA, Gratacós E, *et al.* Matrix metalloproteinases -2 and -9 and their endogenous tissue inhibitors in fetal membrane repair following fetoscopy in a rabbit model. Mol Hum Reprod 2000;6(5):479-85.

17. Kumar D, Fung W, Moore RM, *et al.* Proinflammatory cytokines found in amniotic fluid induce collagen remodelling, apoptotis, and biophysical weakening of cultured human fetal membranes. Biol Reprod. 2006;74:29-34.

18. Parry LJ, Bathgate RA. The role of oxytocin and regulation of uterine oxytocin receptors in pregnant marsupials. Exp Physiol 2000;85:91S–99S.

19. Ou CW, Orsino A, Lye SJ. Expression of connexin-43 and connexin-26 in the rat myometrium during pregnancy and labor is differentially regulated by mechanical and hormonal signals. Endocrinology 1997;138:5398–5407.

20. Kendal-Wright CE. Stretching, mechanotransduction, and proinflammatory cytokines in the fetal membranes. Reprod Sci. 2007;14(8 Suppl):35-41.

21. Mohan AR, Sooranna SR, Lindstrom TM, *et al.* The effect of mechanical stretch on COX-2 expression and AP-1 and NFκB activity in human amnion cells. Endocrinology 2007;148:1850–7.

22. Sooranna SR, Engineer N, Loudon JAZ, *et al.* The mitogen-activated protein kinase dependent expression of prostaglandin H synthase-2 and interleukin-8 messenger ribonucleic acid by myometrial cells: the differential effect of stretch and IL-1β. J Clin Endocrinol Metab. 2005;90:3517-3527.

23. Kanefsky J, Lenbury M, Hai CM. Cholingeric receptor and cyclic stretch-mediated inflammatory gene expression in intact ASM. Am J Respir Cell Mol Biol. 2006;34:417-425.

24. Li LF, Ouyang B, Choukroun G, et al. Stretch-induced IL-8 depends on c-Jun NH2-terminal and nuclear factor-κBinducing kinases. Am J Physiol Lung Cell Mol Physiol.

25. Nemeth E, Millar LK, Bryant-Greenwood GD. Fetal membrane distension: II. Differentially expressed genes regulated by acute distension in vitro. Am J Obstet Gynecol. 2000;182:60-67.

26. McLaren J, Taylor DJ, Bell SC. Prostaglandin E(2)-dependent production of latent matrix metalloproteinase-9 in cultures of human fetal membranes. Mol Hum Reprod. 2000;6(11):1033-40.

27. Bryant-Greenwood G. The extracellular matrix of the human fetal membranes: structure and function. Placenta 1998;19:1-11.

28. Chowdhury B, David AL, Thrasivoulou C, *et al.* Tensile strain increased COX-2 expression and PGE_2 release leading to weakening of the human amniotic membrane. Placenta 2014;35(12):1057-64.

29. Mori R, Power KT, Wang CM, *et al.* Acute downregulation of Cx43 at wound sites leads to a reduced inflammatory response, enhanced keratinocyte proliferation and wound fibroblast migration. J Cell Sci 2006;119:5193–5203.

30. Mendoza-Naranjo A, Cormie P, Serrano AE, *et al.* Overexpression of the gap junction protein Cx43 as found in diabetic foot ulcers can retard fibroblast migration. Cell Biol Int 2012;36(7):661-7.

31. Theodossiou TA, Thrasivoulou C, Ekwobi C, Becker DL. Second harmonic generation confocal microscopy of collagen type I from rat tendon cryosections. Biophys J 2006;91(12):4665-77.

32. Wang CM, Lincoln J, Cook JE, Becker DL. Abnormal connexin expression underlies delayed wound healing in diabetic skin. Diabetes 2007;56:2809–2817.

33. Lee DA, Brand J, Salter DM, *et al.* Quantification of mRNA using real-time PCR and Western blot analysis of MAPK events in chondrocyte/agarose constructs. Methods Mol Biol 2011;695: 77-97.

34. Pfaffl MW, Horgan GW, Dempfle L. Relative expression software tool (REST) for group wise comparison and statistical analysis of relative expression results in real time PCR. Nucleic acids research 2002;30:e3

35. Gratacós E, Devlieger R, Decaluwé H, *et al.* Is the angle of needle insertion influencing the created defect in human fetal membranes? Evaluation of the agreement between specialists' opinions and ex vivo observations. Am J Obstet Gynecol. 2000;182(3):646-9.

36. Gratacós E, Sanin-Blair J, Lewi L, *et al.* A histological study of fetoscopic membrane defects to document membrane healing. Placenta 2006;27(4-5):452-6.

37. Millar LK, Stollberg J, DeBuque L, Bryant-Greenwood G. Fetal membrane distention: determination of the intrauterine surface area and distention of the fetal membranes preterm and at term. Am J Obstet Gynecol 2000;182(1 Pt 1):128-34.

38. Papanna R, Mann LK, Moise KJ Jr, *et al.* Histologic changes of the fetal membranes after fetoscopic laser surgery for twin-twin transfusion syndrome. Pediatr Res 2015;78(3):247-55.

39. Qiu C, Coutinho P, Frank S, *et al.* Targeting connexin43 expression accelerates the rate of wound repair. Curr Biol 2003;30;13(19):1697-703.

40. Wright CS, van Steensel MA, Hodgins MB, Martin PE. Connexin mimetic peptides improve cell migration rates of human epidermal keratinocytes and dermal fibroblasts in vitro. Wound Repair Regen 2009;17(2):240-9.

41. Ruoslahti E, Engvall E. Integrins and vascular extracellular matrix assembly. J Clin Invest 1997;100(11 Suppl):S53-6.

42. Divers MJ, Bulmer JN, Miller D, Lilford RJ. Beta 1 integrins in third trimester human placentae: no differential expression in pathological pregnancy. Placenta 1995;16:245-260.

43. Redd MJ, Cooper L, Wood W, *et al.* Wound healing and inflammation: embryos reveal the way to perfect repair. Philos Trans R Soc Lond B Biol Sci 2004;359(1445):777-84.

44. Wall ME, Otey C, Qi J, Banes AJ. Connexin 43 is localized with actin in tenocytes. Cell Motil Cytoskeleton. 2007;64(2):121-30.

45. Stanley RL, Fleck RA, Becker DL, *et al.* Gap junction protein expression and cellularity: comparison of immature and adult equine digital tendons. J Anat 2007;211(3):325-34.

46. Graham JS, Vomund AN, Phillips CL, Grandbois M. Structural changes in human type I collagen fibrils investigated by force spectroscopy. Exp Cell Res. 2004;299(2):335-42.

47. Eppell SJ, Smith BN, Kahn H, Ballarini R. Nano measurements with micro-devices: mechanical properties of hydrated collagen fibrils. J R Soc Interface. 200622;3(6):117-21.

48. van der Rijt JA, van der Werf KO, Bennink ML, Dijkstra PJ, Feijen J. Micromechanical testing of individual collagen fibrils. Macromol Biosci. 2006;6(9):697-702.

49. Wenger MP, Bozec L, Horton MA, Mesquida P. Mechanical properties of collagen fibrils. Biophys J 2007;93(4):1255-63.

Table 1 | Clinical information for patients undergoing laser ablation therapy

Patient No.	Maternal age	Indication for surgery	GA intervention (weeks+days)	GA delivery (weeks+days)	Time from surgery to delivery (days)	Type of analysis
1	39	TTTS stage I	24+0	35+5	82	IMF & SHG
2	28	TTTS stage I	19+3	29+4	71	IMF & SHG
3	28	FETO for CDH	28+1	32+6	33	IMF & SHG
4	32	TTTS stage III	26+5	26+6	1	IMF & SHG
5	35	TTTS stage II,	24+3	25+3	7	IMF & SHG
6	20	TTTS stage II	18+5	30+1	100	IMF & SHG
7	34	TRAPS	15+0	35+0	140	RT-qPCR
8	33	TTTS stage III	22+2	23+0	5	IMF & SHG
9	29	TTTS stage III	21+6	35+5	97	RT-qPCR
10	36	TTTS stage V	19+3	37+4	145	RT-qPCR
11	33	TTTS stage III	25+3	31+5	44	RT-qPCR
12	29	TTTS stage IV	19+5	29+5	70	IMF & SHG

TTTS: twin-to-twin transfusion syndrome; **FETO**: fetoscopic tracheal occlusion; **CDH**: congenital diaphragmatic hernia; **TRAPS**: twin reversed arterial perfusion sequence; **GA**: gestational age. All pregnancies were delivered by caesarean section.
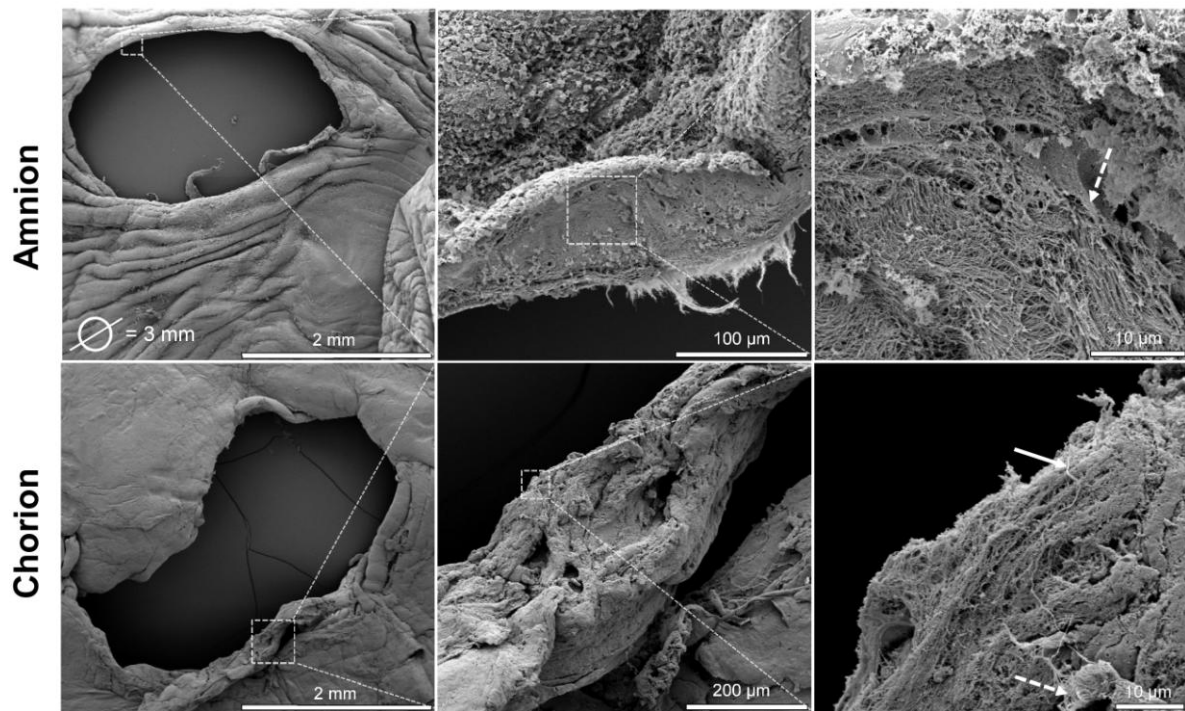
Figure 1. Scanning electron microscopy of fetal membrane defect. Image shows membrane surface and structural details within the amniotic membrane (top panel) and chorionic membrane (bottom panel) after fetoscopic surgery. The fetal membrane was taken from a 28 year old patient who underwent fetoscopic surgery for treatment of stage I twin-to-twin transfusion syndrome at 19 weeks+3 days and who was delivered at 29 weeks+4 days by caesarean section. Scale bar indicated by white lines, with white boxes showing region of higher magnification.
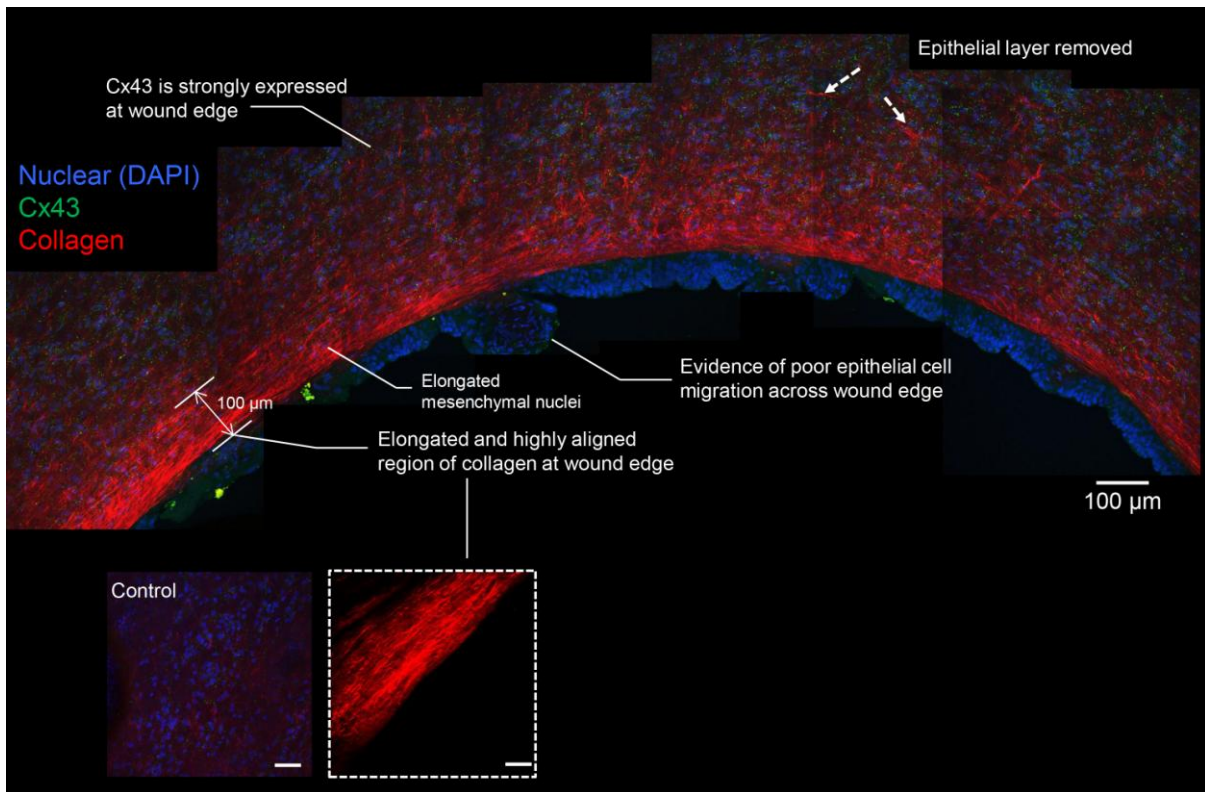
Figure 2. Collagen organisation and Cx43 protein expression in the amniotic membrane. The fetal membrane was taken from a 34 year old patient who underwent fetoscopic laser coagulation in a monochorionic twin pregnancy complicated by twin reversed arterial perfusion. Gestational age at surgical intervention was 15 weeks+0 days and gestational age at delivery by caesarean section was 35 weeks+3 days. Merged images shows Cx43 expression in the fibroblast layer with dense regions of collagen fibres orientated along the length of the fibroblast layer in the wound edge of the amniotic membrane. Nuclei in blue were stained with DAPI and collagen fibres in red indicated by white lines detected by SHG confocal imaging. Inset shows higher magnification of the collagen fibres close to the wound edge. Merged image on left side shows control amniotic membrane taken from the same patient away from the wound. Scale bar = 100 μm.
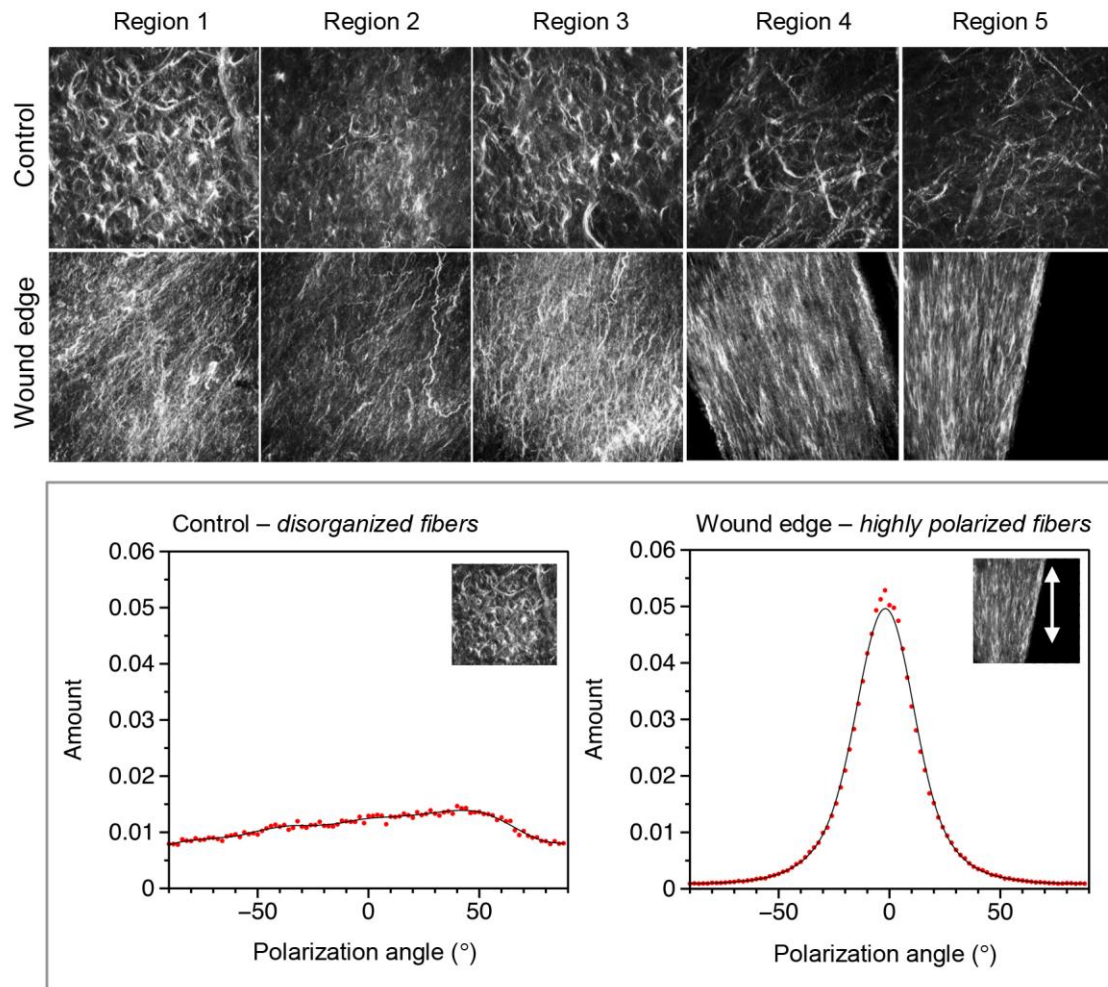
Figure 3. Collagen orientation in the amniotic membrane after fetoscopic surgery. Representative SHG confocal images show orientation of collagen fibres in the five regions of the wound edge and compared to control amniotic membranes taken from the same patient away from the wound (top panel). A distribution of orientation values for each image is shown in the bottom panel with regions of highly polarised fibres in all regions of the wound edge compared to a disorganised arrangement in controls. The fetal membrane was taken from a 29 year old patient who underwent fetoscopic surgery for treatment of stage IV twin-to-twin transfusion syndrome at 19 weeks+5 days and who was delivered at 29 weeks+5 days by caesarean section.
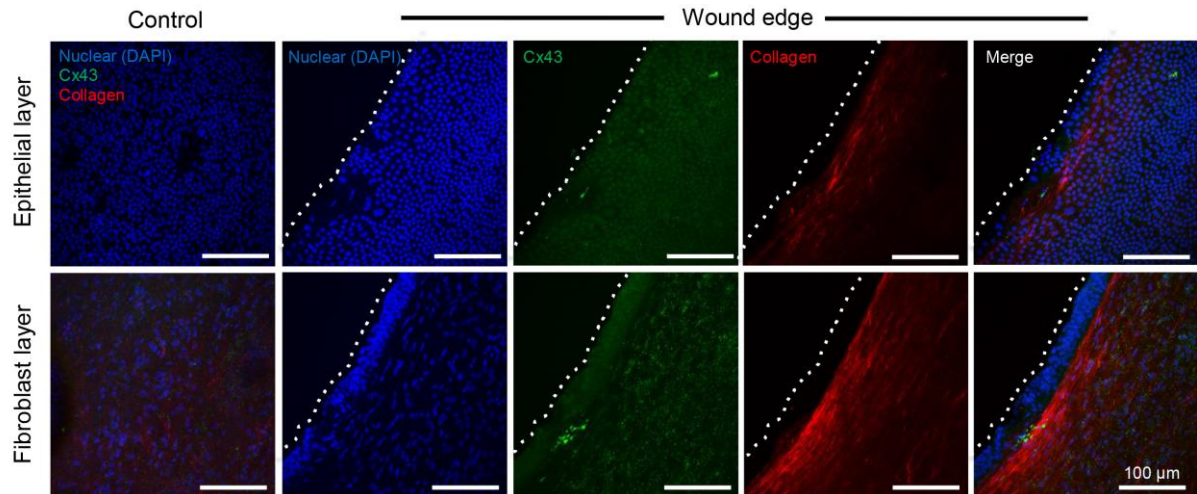
Figure 4. Collagen organisation and Cx43 protein expression in the epithelial and fibroblast layer. Merged images show characteristic spotted staining of Cx43 protein expression in the fibroblast layer of the amniotic membrane with dense regions of collagen fibres aligned in parallel along the wound edge of the amniotic membrane. Blue signal is DAPI staining of nuclei and collagen fibres in red indicated by white lines detected by SHG confocal imaging. The dotted white lines shows the border along the length of the wound edge in the amniotic membrane. Merged image on left side shows control amniotic membrane taken from the same patient away from the wound. Scale bar = 100 μm.
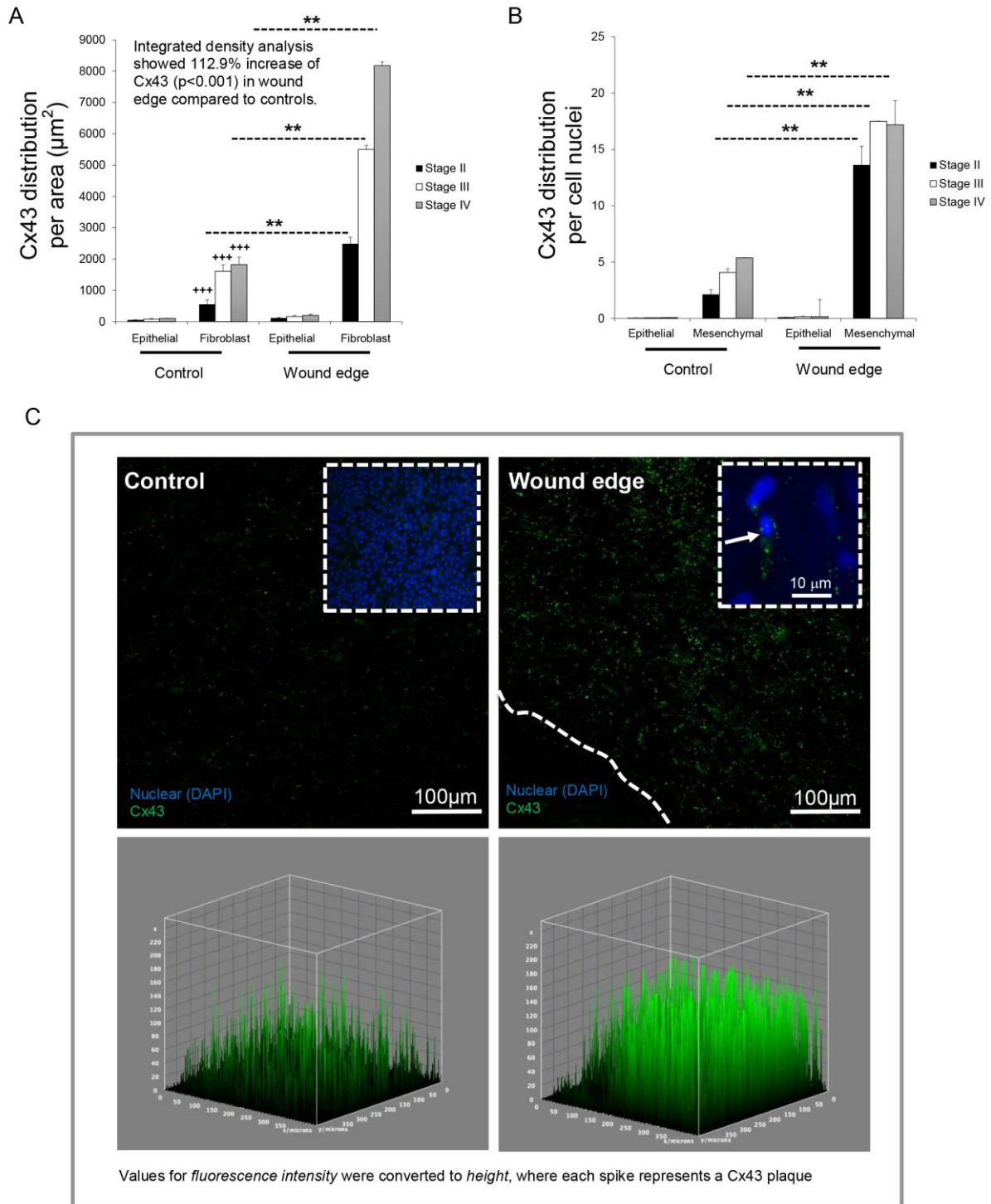
Figure 5: Cx43 distribution and plaque formation in the tissue layers of the amniotic membrane after fetoscopic surgery. The distribution of Cx43 was analysed per unit tissue area for comparisons between epithelial and fibroblast layer (A) and per cell nuclei (B). Integrated density was quantified for cell fluorescence and compared between control and wound edge specimens. For quantification of Cx43 plaque density, each spike represents a Cx43 plaque (C). In all cases, error bars represent the mean and SEM values for n=8 to 10 replicates representing amniotic membranes taken from three patients, where *$p<0.05$, **$p<0.01$ and ***$p<0.001$.
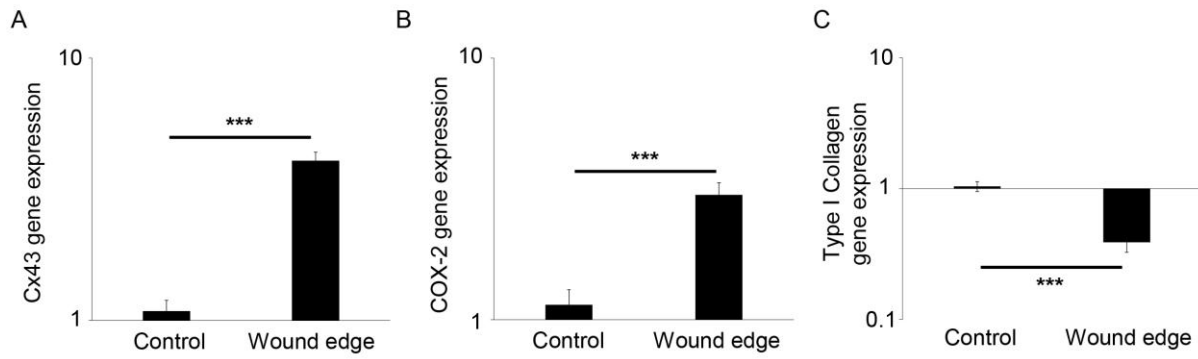
Figure 6. G**ene expression levels in the amniotic membrane after fetoscopic surgery**. Gene expression of Cx43, COX-2 and Type I collagen was presented as ratio values and normalised to control amniotic membranes taken from the same patient away from the wound (B). In all cases, error bars represent the mean and SEM values for n= 12 to 18 replicates representing amniotic membranes taken from three patients, where *p<0.05, **p<0.01 and ***p<0.001.
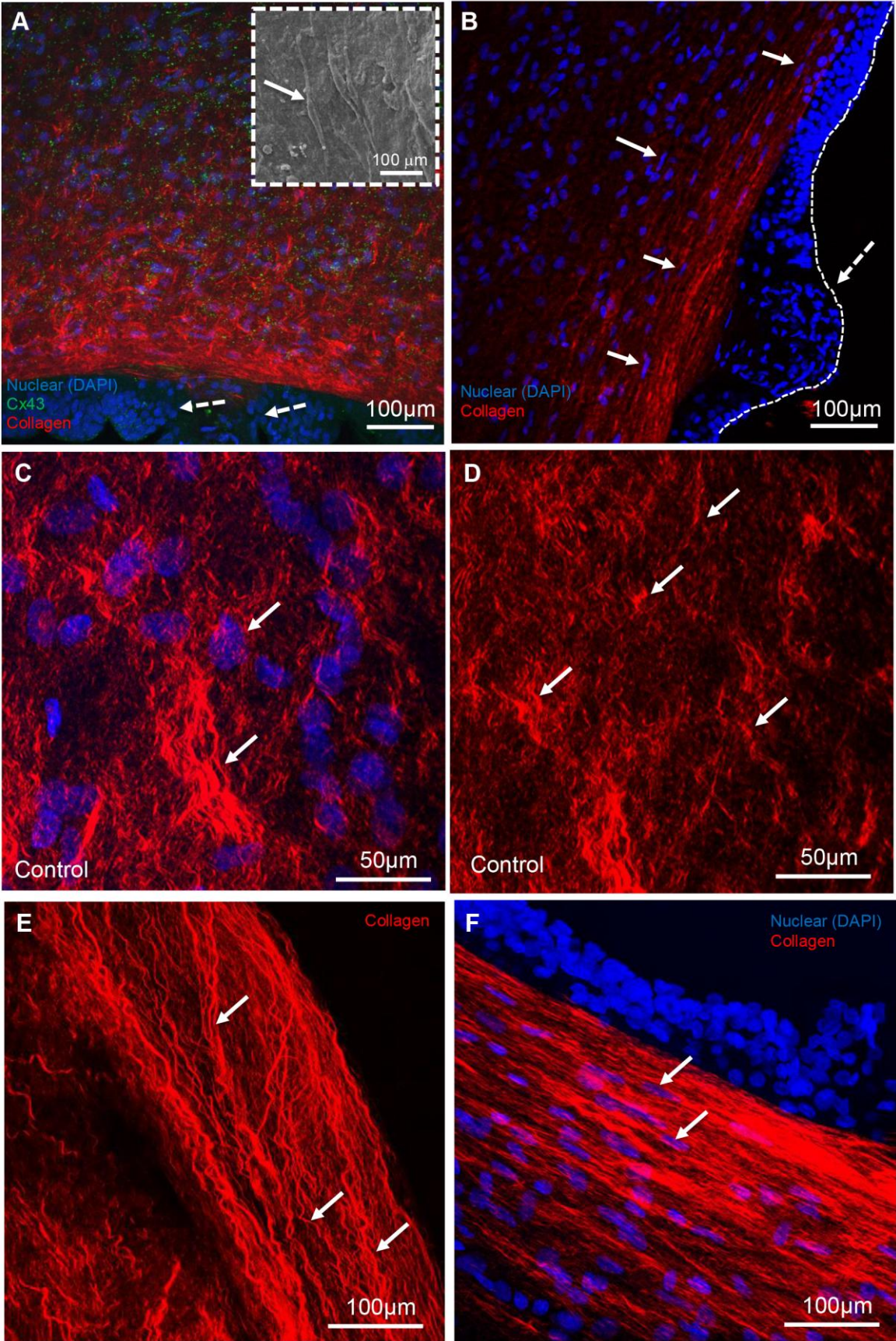
Nuclear (DAPI)
Cx43
Collagen
100 μm
100µm

Nuclear (DAPI)
Collagen
100µm

Control
50µm

Control
50µm

Collagen
100µm

Nuclear (DAPI)
Collagen
100µm

Figure 7. Cell migration and collagen organisation in the fetal membrane defect.
Immunofluoresence confocal microscopy shows bulbous regions of epithelial cells (indicated by white dashed arrows, A, B) and increased Cx43 protein expression (D, E) and collagen alignment at the interface between the fibroblast layer and wound edge of the amniotic membrane (indicated by white arrows). Scanning electron microscopy shows flattened morphology of mesenchymal cells close to the wound edge with characteristic lamellipodium projections (C). Higher magnification shows typical punctate plaques of Cx43 at the cell to cell contacts (E) and densely aligned collagen fibres at the wound edge (F). Inset in D shows negligible Cx43 expression in fibroblast layer in patient matched control amniotic membrane. Wound edge in B and D is indicated by white dashed line. The thickness of the amniotic membrane is approximately 117 μm.